RESEARCH ARTICLE Indian Journal of Animal Research, Volume 59 Issue 7: 1240-1248 (July 2025)

An Ultrastructural Investigation of Spermiogenesis and Sperm Structure in Asian Warty Newt (*Paramesotriton chinensis*)

Zihui Yang[1], Yiyun Mei[2], Liang Xia[2], Shenghao Yao[2], Cangsong Chen[1,2], Jia Yang[1,2]

10.18805/IJAR.BF-1895

ABSTRACT

Background: The Asian warty newt is a rare amphibian species endemic to China and is listed as a second-class national protected wild animal. This study observes the spermiogenesis and sperm ultrastructure of the Asian warty newt and explores the relationship between structure and function, elucidating the male reproductive biology of this rare amphibian at the cellular and molecular levels.

Methods: The collected samples were fixed in 2.5% glutaraldehyde and stored at 4°C. The corresponding electron microscope samples were prepared respectively. The spermiogenesis and ultrastructure changes of spermatids were observed by transmission electron microscopy (TEM) and the morphology and structure of sperms were studied by scanning electron microscopy (SEM).

Result: During spermiogenesis, the morphology and structure of spermatids undergo significant changes, ultimately forming mature sperm with highly condensed chromatin, an elongated nucleus and structures such as the acrosome and tail. The sperm ultrastructure of the Asian warty newt is divided into the head, neck and tail: the head is slender with an acrosome hook; the neck is short and not prominent and the tail is divided into the middle piece, principal piece and end piece. The study found that certain structural features of the sperm are related to its fertilization method and reproductive habits and its morphological structure shares some common characteristics with the sperm of the Salamandridae family.

Key wards: Morphological structure, *Paramesotriton chinensis*, Sperm, Spermiogenesis, Ultrastructure.

INTRODUCTION

The Asian warty newt (*Paramesotriton chinensis*) belongs to the class Amphibia, order Caudata, family Salamandridae and genus *Paramesotriton* (IUCN, 2024; Song *et al*., 2006; Song *et al*., 2010; Lv and Shen, 1998; Lou *et al*., 2022). It is a rare amphibian species endemic to China and is listed as a second-class national protected wild animal. Its distribution is narrow, with records only in Zhejiang and southern Anhui (Liu *et al*., 2019). Over the past decade, human activities such as river sand excavation and electrofishing have severely damaged its habitat and wild populations, leading to a sharp decline in their numbers. Given this urgent situation, it is particularly important to conduct in-depth research on the conservation of the Asian warty newt.

In previous studies, many researchers have investigated its behavioral habits, survival status, endangered condition and genome sequencing analysis (Song *et al*., 2006; Song *et al*., 2010; Lv and Shen, 1998; Yang *et al*., 2017; Tang *et al*., 2022). However, there is a lack of systematic research on the Asian warty newt and no studies on its reproductive biology have been reported. This study uses scanning electron microscopy (SEM) and transmission electron microscopy (TEM) to observe the spermiogenesis and sperm structure of the Asian warty newt, revealing the characteristics of sperm formation and morphology. Based on these findings, the study explores the relationship between structure and function, elucidating the male reproductive biology of this rare amphibian at the cellular and molecular levels. This provides a theoretical basis for the evolution of spermatogenesis patterns and offers insights for both *in situ* and *ex situ* conservation of the Asian warty newt, it is of great significance to its population reproduction. At the same time, as an important part of the ecosystem, the normal reproduction of amphibians helps to maintain the balance of the ecosystem and protect biodiversity.

[1]College of Life Sciences, China Jiliang University, Zhejiang Hangzhou, 310018, China.
[2]Scientific Research Department, Zhejiang Museum of Nature History, Zhejiang Hangzhou, 310013, China.

Corresponding Authors: Cangsong Chen, Jia Yang; College of Life Sciences, China Jiliang University, Zhejiang Hangzhou, 310018, China; Scientific Research Department, Zhejiang Museum of Nature History, Zhejiang Hangzhou, 310013, China.
Email: yangj@zmnh.com

How to cite this article: Yang, Z., Mei, Y., Xia, L., Yao, S., Chen, C. and Yang, J. (2025). An Ultrastructural Investigation of Spermiogenesis and Sperm Structure in Asian Warty Newt (*Paramesotriton chinensis*). Indian Journal of Animal Research. 59(7): 1240-1248. doi: 10.18805/IJAR.BF-1895.

Submitted: 18-09-2024 **Accepted:** 30-10-2024 **Online:**20-12-2024

MATERIALS AND METHODS

This experiment was conducted from 2021-12 to 2024-7 in the Scientific research department of Zhejiang Museum of Nature History.

Sample collection

The Asian warty newt individuals used in this experiment were collected in 2018 from a natural population in Jingning, Lishui, Zhejiang Province (coordinates: 119°63′-119°64′E, 27°76′-27°77′N, altitude 200-400 m). To ensure that the

collected experimental animals were adult males with well-developed gonads, the selection was based on morphological characteristics: adult males possess light-colored papillae on the anterior edge of the cloacal opening, black-brown coloration on the ventral side of the body and lateral sides of the tail, orange-yellow patches of varying sizes in front of the cloaca, small yellow spots scattered on the limbs, a slightly purplish hue on the middle to posterior parts of the tail and orange-red spots on the ventral side of the tail. Considering the small population size of the Asian warty newt in the wild, no repeated sampling was conducted for each developmental stage. However, it was ensured that the selected individuals at each stage were representative of normal gonadal development in adult males. Additionally, individuals with similar body weight and length were chosen to avoid experimental errors due to individual differences.

Three individuals were used for testis collection. The collected samples were dissected on the same day and the testes were fixed in 2.5% glutaraldehyde and stored at 4°C. For sperm collection, seven individuals were temporarily housed in a naturalistic artificial breeding environment at the Zhejiang Museum of Natural History. Sperm samples were collected using the method described by Guo *et al.* (2010) by gently pressing the sides of the newt's abdomen near the cloaca with fingers to collect the white viscous semen that flowed out of the cloaca. The semen was then fixed in 2.5% glutaraldehyde and stored at 4°C. Throughout the process, no harm was done to the animals. Only fixed samples were used for the preparation, observation, photography and analysis under the electron microscope.

The individuals consumed from the natural population in this study will be replenished through the artificial hatching and release of Asian warty newts. The animal experiments and protocol of this study were reviewed and approved by the ethics committee of the China Jiliang University.

Electron microscopy sample preparation

Scanning Electron Microscopy (SEM) Sample Preparation: The samples were rinsed three times with phosphate buffer (0.1 mol. L^{-1}, pH=7.0) for 15 minutes each. They were then fixed with 1% osmium tetroxide at room temperature for 1.5 hours, dehydrated using an ethanol gradient, dried (Hitachi HCP-2 critical point dryer, Japan) and coated (Hitachi GVC-2000 ion sputter, Japan). The samples were then observed and photographed using a scanning electron microscope (Hitachi SU-8010, Japan).

Transmission Electron Microscopy (TEM) Sample Preparation: The samples were rinsed three times with phosphate buffer (0.1 mol. L^{-1}, pH=7.0) for 15 minutes each. They were then fixed with 1% osmium tetroxide at room temperature for 1.5 hours, dehydrated using an ethanol gradient, treated with 90% and 95% acetone solutions for 15 minutes each and pure acetone twice for 20 minutes each. The samples were infiltrated and embedded with Spurr embedding agent, sectioned using an ultramicrotome (LEICA EM UC7, Germany), double-stained with lead citrate and uranyl acetate and observed and photographed using a transmission electron microscope (Hitachi H-7650, Japan).

RESULTS AND DISCUSSION

This study used transmission electron microscopy (TEM) to observe spermiogenesis and sperm ultrastructure and scanning electron microscopy (SEM) to examine sperm morphological characteristics. Spermiogenesis was staged based on changes in chromatin within the nucleus, perinuclear microtubules and acrosome vesicles. Sperm morphology was classified according to distinct features.

Spermatids

Early spermatids

Early spermatids appear nearly round in cross-section, with large nuclei and evenly granular chromatin (Fig 1A). On one side of the nucleus, spherical acrosome vesicles appear, with Golgi apparatus and mitochondria nearby (Fig 1B, C). The area where the acrosome vesicles contact the nucleus shows a slight inward indentation with high electron density, forming an arc-shaped plate (Fig 1B-D). On the opposite side of the acrosome vesicles, a centrosome surrounded by a ring band is visible (Fig 1D). The ring band consists of two parts: a distal lamellar ring with high electron density, situated farther from the nucleus and a proximal granular ring with lower electron density, located closer to the nucleus. The entire structure gradually moves closer to the nucleus (Fig 1J). In the cytoplasm, mitochondria appear vacuolated, with the internal cristae gradually disappearing and moving closer to the cell membrane (Fig 1C).

Mid-stage spermatids

Mid-stage spermatids undergo deformation, with further reduction in volume. The nuclei exhibit longitudinal circular manchette microtubules, causing mechanical compression and deformation of the nucleus. Some chromatin within the nucleus condenses into dense granules (Fig 1G). The perforatorium gradually shifts to one side of the nucleus (Fig 1E, F) and reaches the junction of the acrosome vesicle and the nucleus (Fig 1F-H). The acrosome vesicle becomes wrinkled, with its contents becoming denser and more uniform. The outer membrane of the nucleus develops irregular wavy folds and at the junction with the nucleus, it forms an inward concave shape, resembling an inverted "V" that partially encloses the nucleus (Fig 1F, H). The ends of the "V" shape have higher electron density than the middle. On the opposite side of the acrosome vesicle, an electron-dense nuclear fossa appears, containing the proximal centriole (Fig 1I-K). The flagellum originates from the distal centriole behind the nucleus (Fig 1P) and consists of axial fibers, an undulating membrane, an axoneme and marginal fibers, with the base wrapped by a ring band (Fig 1K). Organelles such as mitochondria, the Golgi

apparatus and the endoplasmic reticulum can be seen in the cytoplasm. The number of mitochondria decreases and they move towards the distal end of the acrosome, with vesicles visible near the Golgi apparatus (Fig 1N).

Late spermatids

In late spermatids, the acrosome and nucleus complete their elongation and the circular manchette disappear. The chromatin within the nucleus becomes highly condensed, appearing as a homogeneous state with high electron density (Fig 1K). Cross-sections reveal intranuclear channels, nuclear ridges and nuclear fossae, with clearly visible microtubules surrounding the nucleus (Fig 1K-M). The proximal granular ring surrounding the base of the flagellum decreases in size, while the distal lamellar ring enlarges (Fig 1I, J, O, P), forming the sperm neck ring band. A small amount of Golgi apparatus and endoplasmic reticulum remain in the cytoplasm (Fig 1L) and mitochondria move to the posterior end of the nucleus to form the mitochondrial sheath of the sperm tail.

Sperm

The sperm of the Asian warty newt consists of three parts: the head, neck and tail. The scanning electron microscopy results show that the sperm is generally slender (Fig 2A). The head is larger than the tail, with a long conical shape and an acrosomal barb (Fig 2B). The neck piece is short and not prominent (Fig 2C). The tail is long and slender, with a curved shape (Fig 2A, E), composed of axial fibers, an undulating membrane and axonemes. The undulating membrane spirally wraps around the axial fibers (Fig 2D).

Head structure

The head of the Asian warty newt sperm consists of the acrosome, perforatorium, nucleus and intranuclear channel. The acrosome contains uniformly dense material, surrounded by a membrane (Fig 3A). In the middle, a long, cylindrical perforatorium extends to the anterior end of the nucleus. The perforatorium is composed of two materials with different electron densities: the central part has lower electron density, while the edges have higher electron

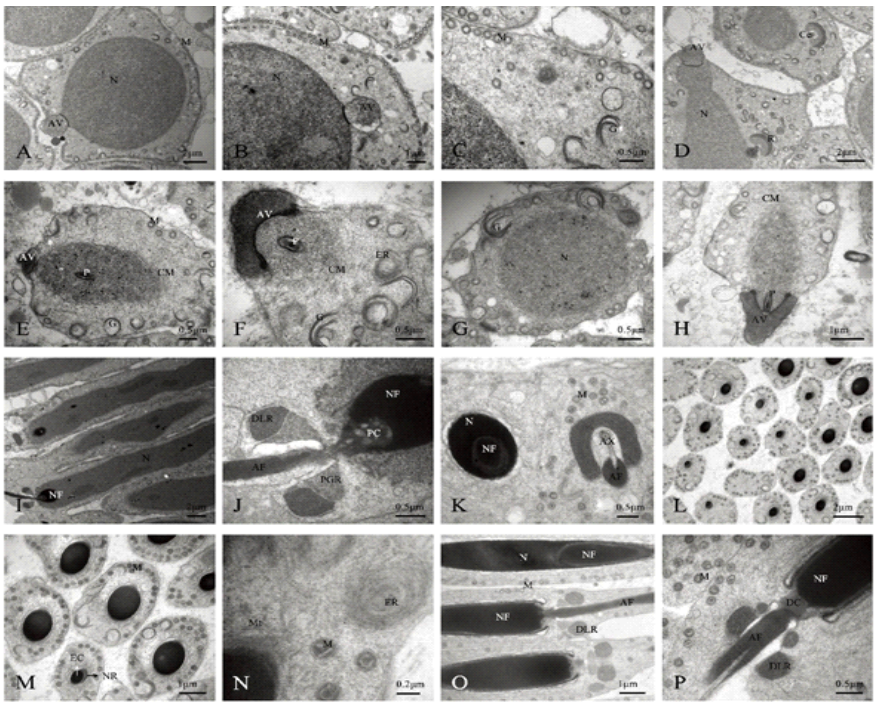

A: Early spermatid, scale bar=2 μm; B: Early spermatid, scale bar=1 μm; C: Early spermatid, scale bar=0.5 μm; D: Early spermatid, scale bar=2 μm; E: Mid-stage spermatid, scale bar=0.5 μm; F: Mid-stage spermatid, scale bar=0.5 μm; G: Mid-stage spermatid, scale bar=0.5 μm; H: Mid-stage spermatid, scale bar=1 μm; I: Mid-stage spermatid, scale bar=2 μm; J: Mid-stage spermatid, scale bar=0.5 μm; K: Late spermatid, scale bar=0.5 μm; L: Late spermatid, scale bar=2 μm; M: Late spermatid, scale bar=1 μm; N: Late spermatid, scale bar=0.2 μm; O: Late spermatid, scale bar=1 μm; P: Late spermatid, scale bar=0.5 μm. AF: Axial fiber; AV: Acrosome vesicle; AX: Axoneme; Ce: Centrosome; CM: Circular manchette; DC: Distal centriole; DLR: Distal lamellar ring; EC: Endonuclear canal; ER: Endoplasmic reticulum; G: Golgi apparatus; M: Mitochondria; Mt: Microtubules; N: Nucleus; NF: Nuclear fossa; NR: Nuclear ridge; P: Perforatorium; PC: Proximal centriole; PGR: Proximal granular ring.

Fig 1: Transmission electron microscopy (TEM) of early spermatid, mid-stage spermatid and late spermatid.

density (Fig 3A). The nucleus is rod-shaped, with uniformly high electron density chromatin. There are cavities at both the anterior and posterior ends of the nucleus: the anterior cavity forms an intranuclear channel and contains the rear part of the perforatorium (Fig 3B-H), while the posterior cavity forms a nuclear fossa, which is an inward indentation

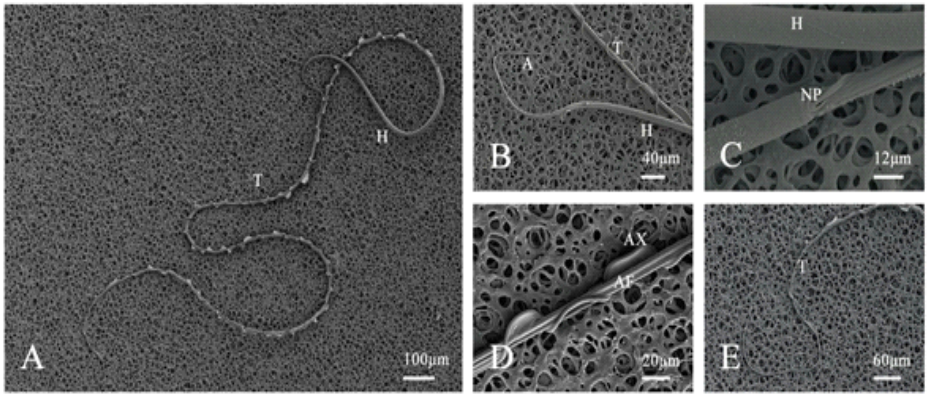

A: The whole sperm, scale bar= 100 μm; B: Sperm head, scale bar= 40 μm; C: Sperm neck piece, scale bar= 12 μm; D: Sperm tail, scale bar= 20 μm; E: The terminal part of sperm tail, scale bar= 60 μm. A: Acrosome; AF: Axial fiber; AX: Axoneme; H: Head; NP: Neck piece; T: Tail.

Fig 2: Scanning electron micrograph (SEM) of sperm.

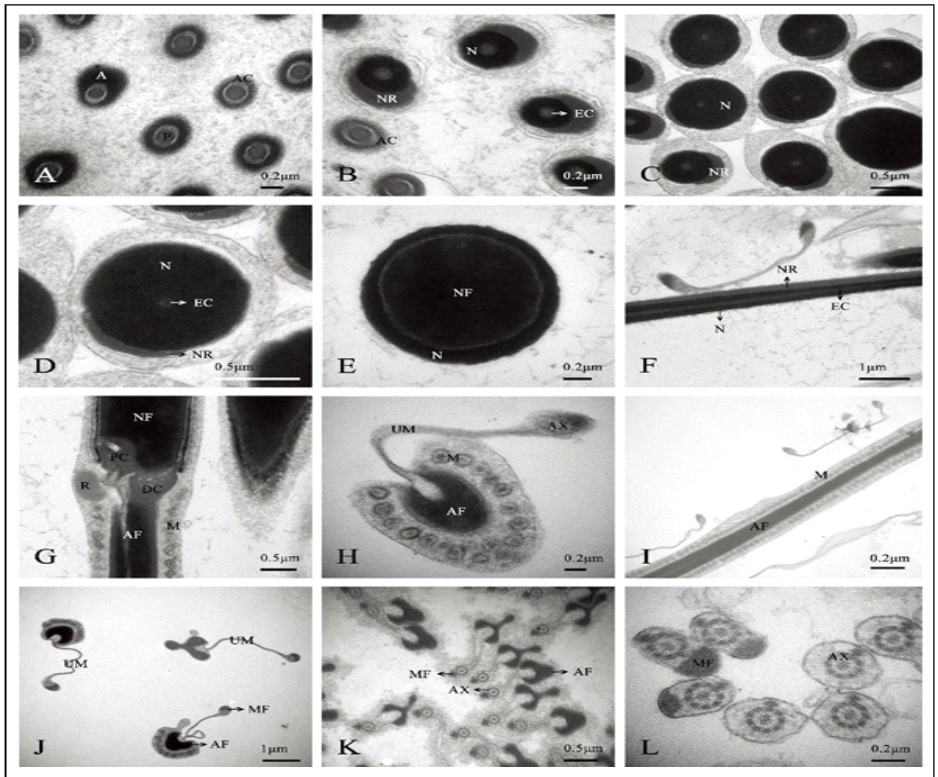

A: Sperm head, scale bar= 0.2 μm; B: Sperm head, scale bar= 0.2 μm; C: Sperm head, scale bar= 0.5 μm; D: Sperm head, scale bar= 0.5 μm; E: Sperm head, scale bar= 0.2 μm; F: Sperm head, scale bar= 1 μm; G: Sperm neck piece, scale bar= 0.5 μm; H: The midpiece of sperm tail, scale bar= 0.2 μm; I: The midpiece of sperm tail, scale bar= 0.2 μm; J: The midpiece and principal piece of sperm tail, scale bar= 1 μm; K: The principal piece of sperm tail, scale bar= 0.5 μm; L: The end piece of sperm tail, scale bar= 0.2 μm. A: Acrosome; AC: Acrosome cone; AF: Axial fiber; AX: Axoneme; DC: Distal centriole; EC: Endonuclear canal; M: Mitochondrion; MF: Marginal filament (juxta-axonemal fiber); N: Nucleus; NF: Nuclear fossa; NR: Nuclear ridge; P: Perforatorium; PC: Proximal centriole; R: Ring; UM: Undulating membrane.

Fig 3: Transmission electron microscopy (TEM) of sperm.

with lower electron density than the nucleus (Fig 3E, G). The nuclear ridge consists of multiple regularly arranged, layered and hollow tubular subunits (Fig 3B-D). It starts at the anterior end of the nucleus, encircling about half of it and appears crescent-shaped in the mid-posterior section, disappearing towards the end of the nucleus (Fig 3B, C). The overall electron density of the nuclear ridge is lower than that of the nucleus and it is surrounded by a membrane. The intranuclear channel disappears (Fig 3C).

Neck structure

The neck of the Asian warty newt sperm connects the head and the tail. Under scanning electron microscopy, the neck appears slightly narrower than the head (Fig 2A). The anterior end, which is the posterior end of the nuclear fossa, indents into the nucleus, forming a smooth, bullet-shaped structure in longitudinal section, composed of material with lower electron density than the nucleus. The proximal centriole and distal centriole are visible at the posterior end, with the proximal centriole oriented towards one side of the neck and the distal centriole towards the base of the neck. They are arranged at an angle, making it difficult to observe both centrioles simultaneously in a cross-section of the neck, but they can be observed together in a longitudinal section at a specific angle. Surrounding the distal centriole, a ring band is observable in the same plane. The electron density of the proximal centriole, distal centriole and ring band is significantly lower than that of the nuclear fossa and the axial fibers of the sperm tail. The sperm tail begins at the distal centriole (Fig 3G).

Tail structure

The sperm tail of Asian warty newt comprises the midpiece, principal piece and end piece.

Midpiece

The midpiece consists of axoneme, mitochondria, undulating membrane, axial fiber and marginal fiber (Fig 3D). The axoneme runs parallel to the central axis of the sperm, with the anterior basal part connecting to the posterior edge of the proximal centriole in the neck and extending to the principal piece of the tail. Mitochondria are arranged in a single layer around the axoneme, numbering approximately 11-15, with a clear membrane structure. The mitochondrial layer is enveloped by a membrane, containing cytoplasm within (Fig 3H, I). The undulating membrane is a membranous structure with cytoplasm in the center, thicker near the axoneme and appears as an elongated trumpet shape in cross-sections under a transmission electron microscope. The axoneme originates from the distal end of the proximal centriole in the neck and has a typical “9+2” structure, consisting of two parallel central microtubules and nine pairs of peripheral microtubules arranged equidistantly in a circle (Fig 3H, L). On the side of the axoneme away from the axial fiber is the marginal fiber with high electron density, which appears crescent-shaped in cross-sections and is surrounded by a membrane (Fig 3H, J).

Principal piece

The principal piece includes the axial fiber, undulating membrane, axoneme and marginal fiber. The axial fiber gradually tapers and is mainly composed of electron-dense fibers. As it extends further from the midpiece of the sperm tail, the axial fiber deforms, taking on a cloverleaf shape in cross-section, without mitochondria on the periphery. Its outer surface is smooth and the marginal fiber beside the axoneme is semi-circular (Fig 3J, K). The structures of the undulating membrane and axoneme are the same as those in the midpiece, while the cross-sectional area of the marginal fiber gradually decreases (Fig 3J).

End piece

The end piece includes the axoneme and marginal fiber. The undulating membrane gradually shortens and disappears, while the axial fiber and marginal fiber become thinner (Fig 3J, L). In cross-section, the marginal fiber transitions from a crescent shape to a small circle before disappearing, leaving only the remnants of the axoneme structure at the very end of the tail (Fig 2E, 3L).

Spermiogenesis in *Paramesotriton chinensis*

Spermiogenesis is the process by which spermatids undergo a series of significant morphological and structural changes to become spermatozoa. This includes nuclear remodeling, acrosome formation, sperm tail formation and the synthesis and secretion of specific proteins (Zhao *et al*., 2013). Different researchers have different staging criteria for spermiogenesis. For example, Xu *et al*. (2006) classified spermiogenesis in the Fujian large-headed frog (*Limnonectes fujianensis*) into early spermatid stage, nuclear condensation stage and sperm maturation stage based on nuclear changes. Sperone *et al*. (2009) divided spermiogenesis in the Italian newt (*Lissotriton italicus*) into early, mid, late and final stages based on changes in the nucleus and certain organelles. In this study, we divided the process of spermiogenesis into early, mid and late stages based on previous research (Xu *et al*., 2006; Sperone *et al*., 2009) and the changes observed in the nucleus and various organelles of *P. chinensis* during spermiogenesis.

The process of spermiogenesis in *P. chinensis* is similar to that in most Caudata (Sperone *et al*., 2009; Barker and Biesele, 1967) and is more complex compared to Anura (Scheltinga *et al*., 2002a, 2002b; Burgos and Fawcett, 1956). Structures such as the acrosomal vesicle (Baccetti *et al*., 1980), which appears early and plays an important role in the acrosomal reaction and sperm penetration of the egg, are not observed in some Anura species (Scheltinga *et al*., 2002a, 2002b; Burgos and Fawcett, 1956). The early centriolar rings with different densities, which manifest as the proximal granule ring and distal lamellar ring in late spermatids, have been found to eventually form the ring structure surrounding the neck of the sperm. Sperone *et al*. (2009) suggested that the elongated form of the ring structure is a derived characteristic

of sperm in the Salamandridae family. Similar ring structures found in the sperm of species from the Hynobiidae family also support this view (Guo *et al.*, 2010; Zheng *et al.*, 2005; Kim *et al.*, 1995).

Morphological characteristics of the acrosome in *Paramesotriton chinensis* sperm

The acrosome is a lysosome-related organelle (LRO) located at the anterior tip of the sperm head, playing a crucial role in fertilization (Berruti *et al.*, 2010; Guyonnet *et al.*, 2012; Yoshinaga *et al.*, 2003). Sperone *et al.* (2009) proposed that the hook-like shape of the sperm acrosome serves an anchoring function. Our observations of *P. chinensis* sperm revealed a similar hook-shaped protrusion on the head acrosome, which is also seen in species from the Plethodontidae (Wortham *et al.*, 1977), Ambystomatidae (Sever and Kloepfer, 1993) and Salamandridae (Selmi *et al.*, 1997) families among Caudata. However, we noted significant differences in the position, shape and length of the acrosome hook among species from different families, supporting Wortham *et al.* (1982) view that there are distinct inter-family differences in the acrosome hook of Caudata sperm.

In contrast, no hook-like structures were found in the acrosomes of species from the Hynobiidae (Guo *et al.*, 2010; Zheng *et al.*, 2005; Kim *et al.*, 1995; Kuramoto *et al.*, 1995) and Cryptobranchidae (Jamieson *et al.*, 1999; Qiao *et al.*, 2016) families. Instead, their acrosomes exhibit various shapes such as cloverleaf or conical forms, highlighting significant inter-family morphological diversity that may serve as a characteristic marker for certain Caudata classifications (Zheng *et al.*, 2005). Additionally, studies on the ultrastructure of some fish sperm and their corresponding egg types (Emel'yanova *et al.*, 2021, Liu *et al.*, 1992, Lin *et al.*, 1998) have shown that sperm from species without an acrosome or similar vesicles on the sperm head have micropyles on their eggs, serving as the sole entry point for the sperm. Conversely, fish species with acrosome structures on the sperm head lack micropyles, suggesting that the acrosome plays an important role in the sperm's ability to penetrate various barriers to fuse with the egg (Lin *et al.*, 1998). Therefore, it can be further inferred that the presence and morphological differences of acrosomes in Caudata sperm are closely related to the complexity of the barriers encountered during sperm-egg fusion.

Structural characteristics of the nucleus ridge in *Paramesotriton chinensis* sperm

Studies have shown that the nuclear ridge is a structure unique to the sperm head of Caudata among vertebrates (Guo *et al.*, 2010; Sperone *et al.*, 2009; Zheng *et al.*, 2005; Kim *et al.*, 1995; Sever and Kloepfer; 1993, Selmi *et al.*, 1997; Jamieson *et al.*, 1999; Zheng *et al.*, 2004; Wang *et al.*, 2012). Closely related Anura sperm lack this structure. Our study found that the nuclear ridge of *P. chinensis* has a unique morphology, characterized by a single thick crescent-shaped structure and 1-2 smaller semicircular structures nearby. These are composed of approximately 2-5 layers of subunit tubules, differing significantly in number, shape and layers from those reported in species of Salamandridae (Sperone *et al.*, 2009; Selmi *et al.*, 1997; Zheng *et al.*, 2004, Wang *et al.*, 2012), Ambystomatidae (Sever and Kloepfer, 1993) and Hynobiidae (Guo *et al.*, 2010; Zheng *et al.*, 2005; Kim *et al.*, 1995; Kuramoto *et al.*, 1995) (Table 1). This further supports the hypothesis by Zheng *et al.* (2004) that there are significant differences in the nuclear ridge of sperm among different species and genera.

Additionally, we found that the nuclear ridge of *P. chinensis* is morphologically similar to that of *Triturus alpestris* (Selmi *et al.*, 1997) and structurally similar to *Echinotriton chinhaiensis* (Zheng *et al.*, 2004), despite the differences in their habitats and reproductive methods compared to *P. chinensis*. This suggests that the morphology and structure of the nuclear ridge in species of the same family but different genera are not directly related to their living environment or reproductive methods. Comparisons among species of Salamandridae (Sperone *et al.*, 2009; Selmi *et al.*, 1997; Zheng *et al.*, 2004; Wang *et al.*, 2012), Ambystomatidae (Sever and Kloepfer, 1993) and Hynobiidae (Guo *et al.*, 2010; Zheng *et al.*, 2005; Kim *et al.*, 1995; Kuramoto *et al.*, 1995) show that the interspecies

Table 1: The nuclear ridge of *Paramesotriton chinensis* sperm compared with other species of caudata.

Species	Number of nuclear ridges	Nuclear ridge morphology	Nuclear ridge layer	Data resource
Echinotriton chinhaiensis	Multiple	Semicircle	2-5	Zheng *et al.*, 2004
Salamandrina terdigitata	Single	Semicircle	3-9	Selmi *et al.*, 1997
Triturus alpestris	Single	Meniscus	2-5	Selmi *et al.*, 1997
Cynops orientalis	Single	Semicircle		Wang *et al.*, 2012
Lissotriton italicus	Single	Semicircle	2-6	Speron *et al.*, 2009
Taricha granulosa	Single	Crescent		Selmi *et al.*, 1997
Ambystoma opacum	Single	Elliptic		Sever *et al.*, 1993
Batrachuperus longdongensis	Single	Small tubular	1	Zheng *et al.*, 2005
Hynobius leechii	Single	Bundled tubules	1	Kim *et al.*, 1995
Hynobius guabangshanensis	Single	Small tubular	Multilayer	Guo *et al.*, 2010
Paramesotriton chinensis	Multiple	Thick crescent	2-5	This study

differences in nuclear ridge morphology are smaller within genera but larger between families. This indicates a correlation between the nuclear ridge morphology and phylogenetic relationships among Caudata species (Jetz *et al*., 2018). The morphology and number of nuclear ridges are valuable for family and genus identification and species classification in Caudata (Zheng *et al*., 2004).

Given that the unique structures of sperm are often related to their fertilization mechanisms, as discussed earlier regarding the acrosome structure, it is speculated that the nuclear ridge may play a role during the sperm-egg fusion stage. However, whether the nuclear ridge affects sperm-egg fusion and its specific mechanism remains unknown and requires further research.

Mitochondria in *paramesotriton chinensis* sperm

The length of the sperm tail usually accounts for more than 50% of the total sperm length and sperm length is a key indicator of sperm quality (Byrne *et al*., 2003; Pizzari *et al*., 2009; Bhat and Sharma, 2020; Deshmukh *et al*., 2021; Huang *et al*., 2024). Studies have indicated that longer sperm tails are generally associated with higher sperm quality (Cheng *et al*., 2021, 2023). This is because sperm with longer tails typically contain abundant mitochondria, which provide sufficient energy for sperm motility (Byrne *et al*., 2003; Pizzari *et al*., 2009), thereby enhancing sperm quality. Therefore, the mitochondrial content in the sperm tail is considered an important factor influencing sperm quality and competitiveness in sperm competition (Cheng *et al*., 2023); Selmi *et al*. (1997) found that terrestrial species of the Salamandridae family have higher mitochondrial content in their sperm compared to aquatic species, likely due to the higher viscosity of the cloaca in terrestrial species, suggesting that the number of mitochondria in sperm may be closely related to the environmental conditions and energy required for movement (Zheng *et al*., 2005).

Our study found that the mitochondria in *P. chinensis* sperm are located in the midpiece of the tail, similar to internally fertilizing species in the Plethodontidae (Wortham *et al*., 1977); Salamandridae (Sperone *et al*., 2009; Selmi *et al*., 1997; Zheng *et al*., 2004; Wang *et al*., 2012) and Ambystomatidae (Sever and Kloepfer, 1993) families. These mitochondria are spherical and arranged in a single layer around the axial fiber. In contrast, in externally fertilizing species of the Cryptobranchidae (Qiao *et al*., 2016) and Hynobiidae (Guo *et al*., 2010; Zheng *et al*., 2005; Kim *et al*., 1995; Kuramoto *et al*., 1995) families, mitochondria are found in small cytoplasmic granules in the sperm head. This indicates that there are significant differences in the position of mitochondria in the sperm of Caudata species with different fertilization methods. This suggests that during the evolution of Caudata, the differentiation of sperm mitochondrial characteristics may be related to fertilization methods and reproductive habits. However, the specific influencing factors and mechanisms still require further research to be elucidated.

CONCLUSION

The results of this study complement existing knowledge of *P. chinensis* and enable us to identify the ultrastructure of spermiogenesis and sperm in *P. chinensis*. The study found that certain structural features of the sperm are related to its fertilization method and reproductive habits and its morphological structure shares some common characteristics with the sperm of the Salamandridae family.

ACKNOWLEDGEMENT

The present study was funded by the Natural Science Foundation of Zhejiang, grant number LTGS23C030003 and LGN19C040002.

Disclaimers

The views and conclusions expressed in this article are solely those of the authors and do not necessarily represent the views of their affiliated institutions. The authors are responsible for the accuracy and completeness of the information provided, but do not accept any liability for any direct or indirect losses resulting from the use of this content.

Informed consent

The animal experiments and protocol of this study were reviewed and approved by the ethics committee of the China Jiliang University.

Conflict of interest

The authors declare that there are no conflicts of interest regarding the publication of this article. No funding or sponsorship influenced the design of the study, data collection, analysis, decision to publish, or preparation of the manuscript.

REFERENCES

Baccetti, B., Bigliardi, E., Burrini, A.G. (1980). The morphogenesis of vertebrate perforatorium. *Ultrastruct Res*. **71:** 272-87.

Barker, K.R., Biesele, J.J. (1967). Spermateleosis of a salamander Amphiuma tridactylum Cuvier. A correlated light and electron microscope study. *Cellule*. **67:** 91-118.

Berruti, G., Ripolone, M., Ceriani, M. (2010). USP8, a regulator of endosomal sorting, is involved in mouse acrosome biogenesis through interaction with the spermatid ESCRT-0 complex and microtubules. *Biol. Reprod.* **82:** 930-939.

Bhat, Y., Sharma, M. (2020). X-sperm enrichment of bovine semen by percoll density gradient method and its effect on semen quality, sex ratio and conception rate. *Indian Journal of Animal Research*. **54(10):** 1181-1187. doi: 10.18805/ijar.B-3823.

Burgos, M.H., Fawcett, D.W. (1956). An electron microscope study of spermatid differentiation in the toad, Bufo arenarum Hensel. *J. Biophys Biochem Cytol.* **2:** 223-240.

Byrne, P.G., Simmons, L.W., Roberts, J.D. (2003). Sperm competition and the evolution of gamete morphology in frogs. *Proc. Biol. Sci.* **270:** 2079-86.

Cheng, Y.M., Shu, X.X., Zhang, K., Zhu, Y.D., Gong, Y.Z., Xiao, L.Y., Shu, G.C., Xie, F. (2021). The smaller Taliang crocodile newt (*Liangshantriton taliangensis*) invests more in sperm quality to gain advantage in post-copulatory sperm competition. *Chin J. Appl. Environ. Biol.* **27:** 831-836.

Cheng, Y.M., Zhang, K., Liang, F.X., He, L.Y., Zhu, Y.D., Yu, H.Q., Xiao, L.Y., Zheng, P.Y., Xie, F. (2023). Sperm morphological change of *Liangshantriton taliangensis* under different sampling methods. *Chin. J. Zool.* **58:** 554-562.

Deshmukh, B., Verma, A., Gupta, I.D., Kashyap, N. and Saikia, J. (2021). SNP identification in sperm associated antigen 11B Gene and its association with sperm quality traits in Murrah Bulls. *Indian Journal of Animal Research*. **55(9):** 1005-1009. doi: 10.18805/IJAR.B-4152.

Emel'yanova, N.G., Pavlov, D.A. (2021). Features of oogenesis and spermatozoa ultrastructure in the fishes of the genera *Parascorpaena* and *Scorpaenopsis* (Scorpaenidae). *J. Ichthyol.* **61:** 912-922.

Guo, K.J., Mi, X.Q., Deng, X.J. (2010). Morphological Structure of the Spermatozoa in *Hynobius guabangshanensis* (Urodela: Hynobiidae). *Life Sci. Res*. **14:** 38-43.

Guyonnet, B., Zabet-Moghaddam, M., SanFrancisco, S., Cornwall, G.A. (2012). Isolation and proteomic characterization of the mouse sperm acrosomal matrix. *Mol. Cell Proteomics.* **11:** 758-774.

Huang, Y., Gong, T., Meng, L. J., Wu, G., Wang, W.Y., Xu, H.Q., Chen, X., Gao, Y., Feng, X.Z. (2024). Evaluation of the congjiang Xiang Pig's sperm quality by flow cytometry. *Indian Journal of Animal Research*. **58(4):** 573-578. doi: 10.18 805/IJAR.BF-1650.

IUCN. The IUCN Red List of Threatened Species. (2024) Partners Available at: https://www.iucnredlist.org/ (accessed 10 Sep 2024).

Jamieson, B.G.M. (1999). Spermatozoal phylogeny of the Vertebrata. In: The Male Gamete from Basic Science to clinical Applications. [Gagnon, C. (ed)], Cache. River Press. pp. 303-331.

Jetz, W., Pyron, R.A. (2018). The interplay of past diversification and evolutionary isolation with present imperilment across the amphibian tree of life. *Nat. Ecol. Evol*. **2:** 850-858.

Kim, K.H., Park, W.H., Lee, Y.H. (1995). Ultrastructure of Spermatozoa in Urodeles, *Hynobius leechii* (Amphibia: Urodela). *Electron Microspocy*. **25:** 111-121.

Kuramoto, M. (1995). Scanning electron microscopic studies on the Seprmatozoa of same Japanese salamanders (Hynobiidae: Cryptobranchidae: Salamandridae). *Japan. J. Herpetol*. **16(2):** 49-58.

Lin, G.H., Lin, Q., Hu, C.Y., Hong, Y.J. (1998). Comparatively Studies on the Ultrastructures of the Spermatozoon of the Grass Carp, the singuo red carp and the catfish. *J. Nanjing Univ. Nat. Sci*. 90-94.

Liu, R.L., Zhou, J.J., Liu, K.C., Jin, W., Ye, W.J., Xu, X.X. (2019). *Paramesotriton aurantius* (Caudata: Salamandridae) Found in Zhejiang Province. *Chin. J. Zool*. **54:** 117-122.

Liu, Y., Zhang, X.J. (1992). Types of sperm structure and corresponding types of ovum structure. *Acta Sci. Nat. Univ. Norm. Hunan.* 168-174.

Luo, T., Yan, S.S., Xiao, N., Zhou, J.J., Wang, X.L., Chen, W.C., Deng, H.Q., Zhang, B.W., Zhou, J. (2022). Phylogenetic analysis of combined mitochondrial genome and 32 nuclear genes provides key insights into molecular systematics and historical biogeography of Asian warty newts of the genus *Paramesotriton* (Caudata: Salamandridae). *Zool. Res*. **43:** 787-804.

Lv, J.H., Shen, Y.H. (1998). Study on the Behavior and Habits of *Paramesotrition chinensis*. *J. Huaihua Teachers College*. pp. 55-58.

Pizzari, T., Parker, G.A. (2009). Sperm competition and sperm phenotype. Sperm Biology: An Evolutionary Perspective. *Sperm Biology.* 207-245.

Qiao, Z.G., Shen, F.F., Liu, S.Y. (2016). Study on the Spermatozoon Structure of Andrias davidianus. *Sichuan J. Zool*. **35:** 534-540.

Scheltinga, D.M., Jamieson, B.G.M., Bickford, D.P., Garda, A.A., Bao, S.N., Mcdonald, K.R. (2002b). Morphology of the spermatozoao of the Microhylidae (Anura Amphibia). *Acta Zoologica* (*Stockholm*). **83:** 263-275.

Scheltinga, D.M., Jamieson, B.G.M., Mcdonald, K.R. (2002a). Ultrastnicture of the spermatozoa of *Litoria longirostris* (Hylidae, Anura, Amphibia) modifications for penetration of a gelatinous layer surrounding the arboreal egg clutch. *Mem. Queensl. Mus*. **48:** 215-220.

Selmi, M.G., Brizzi, R., Bigliardi, E. (1997). Sperm morphology of salamandrids (Amphibia, Urodela): implications for phylogeny and fertilization biology. *Tissue Cell*. **29:** 651-664.

Sever, D.M., Kloepfer, N.M. (1993). Spermathecal cytology of *Ambystoma opacum* (Amphibia: Ambystomatidae) and the phylogeny of sperm storage organs in female salamanders. *J. Morphol*. **217:** 115-127.

Song, Y.Z., Chen, C.Q., Huang, X.F. (2006). A new record of *Paramesotriton chinensis* in Jiangxi province. *Zool. Res*. **27(6):** 605-606.

Song, Y.Z., Zhang, J.H., Cheng, Y., Huang, X.F., He, L.Z. (2010). Investigate the Rare Animals Resources in the Qixiling Natural Reserve. *Chin. Agri. Sci. Bull*. **26:** 141-143.

Sperone, E., Bonacci, A., Brunelli, E., Tripepi, S., Jamieson, B.G.M. (2009). Male reproductive system in the Italian newt *Lissotriton italicus* (Peracca 1898) (Amphibia, Urodela): ultrastructural and morphological study with description of spermiogenesis, spermatozoon and spermatophore. *Zoomorphology*. **128:** 183-195.

Tang, X., Liang, G.N., Liu, Y.L., Duan, Z.G. (2022). Analysis of transcriptome sequencing and active peptide from the salamander *Paramesotriton chinensis* skin. *J. Anhui Agric. Univ*. 49: 69-75.

Wang, D.H., A. (2012). The Mechanism of Germ Cell Apoptosis during Spermatogenesis of *Cynops orientalis* and the Functions of KIFC1 in Spermiogenesis. [Doctoral dissertation, Zhejiang University, Hangzhou, China].

Wortham, J.W., Brandon, J.A., Martan, J. (1977). Comparative morphology of some plethodontid salamander spermatozoa. *Copeia*. pp. 666-680.

Wortham, J.W., Murphy, J.A., Martgan, J., Brandon, R.A. (1982). Scanning electron microscopy of some salamander spermatoza. *Copeia*. pp. 52-60.

Xu, J.C., Tang, X.S., Fei, C.Y. (2006). A Preliminary Study on Spermiogenesis of *Limnonectes fujianensis*. *J. Huangshan Univ*. pp. 61-63.

Yang, J., Yu, L.P., Zhang, S.Y., Liu, R.L., Chen, C.S., Lin, H.D. (2017). The complete mitochondrial genome of *Paramesotriton chinensis* (Caudata: Salamandridae) and phylogenetic studies of Paramesotriton. *Mitochondrial DNA B Resour*. **2:** 289-290.

Yoshinaga, K., Toshimori, K. (2003). Organization and modifications of sperm acrosomal molecules during spermatogenesis and epididymal maturation. *Microsc. Res. Tech*. **61:** 39-45.

Zhao, B., Ito, K., Iyengar, P.V., Hirose, S., Nakamura, N. (2013). MARCH7 E3 ubiquitin ligase is highly expressed in developing spermatids of rats and its possible involvement in head and tail formation. *Histochem. Cell Biol.* **139:** 447-460.

Zheng, Z.H., Jiang, J.P., Xie, F. (2005). Ultrastructure of the spermatozoa of Longdong stream salamander *Batrachuperus longdongensis* (Urodela: Hynobiidae). *Acta Zool. Sin*. 703-709.

Zheng, Z.H., Xie, F., Jiang, J.P., Fei, L. (2004). Spermatozoa structure of the Chinhai salamander *Echinotriton chinhaiensis* (Caudata: Salamandridae). *Acta Zool. Sin*. 622-629.